# Journal of Materials Chemistry A

Accepted Manuscript






ROYAL SOCIETY OF CHEMISTRY

www.rsc.org/materialsA

Journal Name

RSCPublishing

ARTICLE

# Fabrication of a highly sensitive surface-enhanced Raman scattering substrate for monitoring of the catalytic degradation of organic pollutants

Cite this: DOI: 10.1039/x0xx00000x

Received 00th January 2012,
Accepted 00th January 2012

DOI: 10.1039/x0xx00000x

www.rsc.org/

Wei Song,[a,b] Wei Ji,[a] Sanpon Vantasin,[a] Ichiro Tanabe,[a] Bing Zhao*[b] and Yukihiro Ozaki*[a]

In this paper, we demonstrate a simple and reliable two-step strategy based on an electrospinning technique combined with in situ calcination for the fabrication of ZnO nanofibers deposited on a silver foil surface. These nanofibers are used as a novel sensitive surface-enhanced Raman scattering (SERS) substrate. The strong interactions between ZnO nanofibers and silver foil afford continuous delocalized surface plasmons, resulting in localization of the electric field at the gap between ZnO nanofibers and silver foil; thus, the exciton–plasmon interactions between ZnO nanofibers and the silver foil surface contribute to the enhanced scattering, generating a large electromagnetic field enhancement. In addition, the ZnO nanofibers deposited on the silver foil surface exhibit enhanced photocatalytic activity toward the degradation of organic pollutants because of the charge separation effect and increase in the lifetime of the photogenerated excitons under ultraviolet light irradiation; thus, this new substrate can be used as a SERS substrate for determining the catalytic activity and reaction kinetics during the photodegradation of organic pollutants.

## Introduction

Surface-enhanced Raman scattering (SERS) has become one of the most powerful spectroscopic techniques in the past decades, and has been widely used in diverse areas of chemistry, material sciences, and certain biosciences.[1–6] Compared with conventional spectroscopic techniques such as UV-vis absorption, infrared, and normal Raman spectroscopy, SERS provides an obvious advantage of highly sensitive detection.[7–14] In general, SERS enhancement is usually observed on SERS-active substrates such as roughened coinage metals with well-controlled nanostructures (e.g., Au, Ag, and Cu).[15-17] Recently, semiconductors, quantum dots (QDs), and graphene have also been found to act as Raman signal-enhancing agents.[18–29] Among them, semiconductors have advantages such as adjustable band gaps, stable exciton production, control of stoichiometry, and long-term stability, making them good candidates for SERS substrates. There are two traditional enhancement mechanisms to describe the SERS effect on a metallic substrate: electromagnetic (EM) and chemical enhancement. The EM enhancement is related to the increase in the electric field caused by the surface plasmon resonances of the nanosized metal under laser light. However, the plasmon resonance frequency of semiconductors usually appears in the infrared region, which is quite far from the typically used excitation wavelength range. Therefore, the enhancement in semiconductor substrates may be attributed to the change-transfer (CT) mechanism, with transfer occurring from the semiconductor to the adsorbed molecules. For example, a strong SERS signal from absorbed molecules observed on the ZnO nanocrystal substrate is attributed to the CT contribution.[18] In addition, maximum enhancement of the phonon modes is observed in CdTe QDs upon adsorption of 4-mercaptopyridine (4-MPy) molecules, which is similarly ascribed to the contribution from CT and exciton resonances coupled with the excitation laser.[19] However, the EF of a semiconductor substrate based on such a CT mechanism is relatively low.

In the past two decades, one-dimensional (1-D) semiconductor nanomaterials have attracted extensive attention at the forefront of nanotechnology research owing to their unique electronic, physical, and chemical properties, as well as their wide applications in photocatalysis, plasmon-enhanced spectroscopy, biotechnology, and optoelectronic devices.[30,31] 1-D semiconductor nanomaterials exhibit rich physical properties that can be attributed to the enhanced light–matter interactions and coupling of optical modes to electronic resonances.[32] In addition, 1-D semiconductor nanomaterials, after coupling with noble metal nanoparticles, are good SERS substrate candidates owing to the confinement of light.[33,34] We have studied the SERS properties of 4-MPy adsorbed on the surface of $TiO_2$ nanofibers decorated with silver nanoparticles, and the SERS enhancement can be attributed to long-range EM

enhancement.[35] In addition, 1-D semiconductor arrays decorated with metal nanoparticles have proved to be highly sensitive SERS substrates because many more "gaps" are formed on these structures. For example, controllable heterostructures consisting of ZnO nanorod arrays with attached Ag nanoparticles have been fabricated through a convenient galvanic reduction method and the as-prepared ZnO/Ag nanorod arrays exhibited sensitive detection of *p*-aminothiophenol (PATP) molecules with a limit of detection of $10^{-7}$ M.[36] Vertically aligned Au-coated ZnO nanorods have also been studied for ultrasensitive Raman analyses, in which the detection limit for methylene blue (MB) molecular probes goes down to $1 \times 10^{-12}$ M.[37] However, most of the approaches for the fabrication of noble metal-modified semiconducting ZnO nanomaterials are complicated.

On the other hand, the SERS-active substrates based on noble metal-decorated semiconductor nanomaterials have recently been developed to monitor in situ interfacial catalytic chemical reactions, providing new insights into the kinetics of heterogeneous catalysis.[38] For example, Kang, Shao, and co-workers demonstrated the fabrication of a ZnO–RGO–Au nanocomposite that could be employed as a photocatalyst and SERS substrate for the in situ quantitative monitoring of pollutant (Rhodamine 6G) degradation.[39] Recently, $Ag/TiO_2$ colloid nanocomposites have also been used to monitor the catalytic reduction of 4-nitrophenol under UV irradiation, providing evidence for the photocatalytic effect on the adsorbate under UV irradiation.[40]

In this paper, we demonstrate a facile approach to the fabrication of ZnO nanofibers deposited on a silver foil surface through an electrospinning technique combined with in situ calcination. The as-prepared ZnO nanofibers deposited on the silver foil surface exhibits an excellent SERS property with an outstanding EF of about $1.2 \times 10^8$, which is a high value for a semiconductor substrate. Enhancement of the Raman signal should be due to confinement of light by the underlying plasmonic silver foil with ZnO nanofibers. Furthermore, the as-prepared ZnO nanofibers deposited on the silver foil surface can be employed for SERS monitoring of the photocatalytic degradation of MB molecules under UV light. The use of semiconducting nanofibers coupled with a noble metal may extend the SERS investigation to the photocatalytic degradation of other types of pollutants.

## Experimental section

### Materials.

Silver foil (0.025 mm thick, annealed, 99.95% (metal basis)) was purchased from Alfa Aesar. Polyvinylpyrrolindone (PVP) (Mw = 1,300,000 g $mol^{-1}$) was purchased from Aldrich. Zinc acetate dihydrate (AR) was purchased from Tianjin Guangfu Fine Chemical Research Institute in China. PATP (Wako 1st grade) was purchased from Wako Pure Chemical Industries, Ltd in Japan. MB hydrate was purchased from TCI in Japan. Ethanol was purchased from Chemical Reagent Beijing Co., Ltd. in China and used without further purification.

### Prepararion of ZnO nanofibers deposited on the surface of the silver foil

In a typical procedure, 0.36 g of $Zn(Ac)_2$ was dissolved in 1.4 g of water, followed by the addition of a mixture of 0.25 g of PVP and 2 g of ethanol. The solution was magnetic stirring for more than 1 h. After that, electrospinning was carried out at room temperature. The as-prepared homogenous solution was electrospun using a needle at an applied voltage of 12 kV over a collection distance of 12 cm. The fibers were collected on silver foil and then calcined under air atmosphere at 450 $^oC$ for 3 h in order to remove the PVP and produce ZnO nanofibers on the surface of silver foil. The content of the ZnO nanofibers on the surface of silver foil was controlled by the electrospinning time. The samples for SERS measurements were obtained with an electrospinning time of about 30 min.

### Characterization.

The morphology of the ZnO nanofibers deposited on the surface of the silver foil were characterized using JEOL JSM-6700F field emission scanning electron microscope (FE-SEM) operated at 3.0 kV. TEM images of the ZnO nanofibers were characterized by JEOL JEM-2100F measurement. UV-vis absorption spectra were recorded on a Shimadzu UV-3600 spectrometer. X-Ray diffraction (XRD) patterns were obtained with a PANalytical B.V. (Empyrean) diffractometer using Cu Kα radiation. Analysis of the X-Ray photoelectron spectra (XPS) was performed on an ESCLAB MKII using Al as the exciting source. Raman spectra were obtained with a LabRAM ARAMIS SmartRaman Spectrometer, the 514.5 nm radiation from the Ar+ ion laser (Spectra Physics ) was used as exciting source; the laser power at the sample position was typically 1.0 mW; data was acquired with one 5 s accumulation.

### Catalytic measurement

In a typical catalytic experiment, a piece of silver foil deposited by ZnO nanofibers (about 3 mm×3 mm) was put into 200 μL of MB solution (3.2 mg/L) under UV light. A Hg–Xe lamp (Luminar Ace LA-300UV, Hayashi Watch Works) equipped with a UV-pass filter (wavelength = 280–410 nm) was used as the UV light source. The catalytic activity measurements were conducted in time course mode by monitoring the SERS spectra of the final product.

## Results and discussion

Figures 1a and b show the scanning electron microscopy (SEM) images of ZnO nanofibers deposited on a silver foil surface using electrospinning combined with calcination. It can be seen from the image that the as-prepared ZnO nanofibers are deposited in a disordered manner on the silver foil surface. The diameters of the deposited electrospun ZnO nanofibers are in the 100–200 nm range. The magnified SEM image shows that the as-prepared ZnO nanofibers are composed of many compact ZnO nanoparticles, with sizes ranging from several nanometers to a few tens of nanometers. In addition, the SEM images also show that, in regions without ZnO nanofiber deposition, the silver foil surface is relatively smooth. Transmission electron microscopy (TEM) was used to investigate the fine structure of the ZnO nanofibers. The TEM images (Figure 1c) show that the obtained ZnO nanofibers are composed of many compact ZnO nanoparticles, which is in accordance with the SEM images. The high-resolution TEM (HRTEM) image of a small region of the ZnO nanofiber clearly demonstrates lattice fringes, and the



 

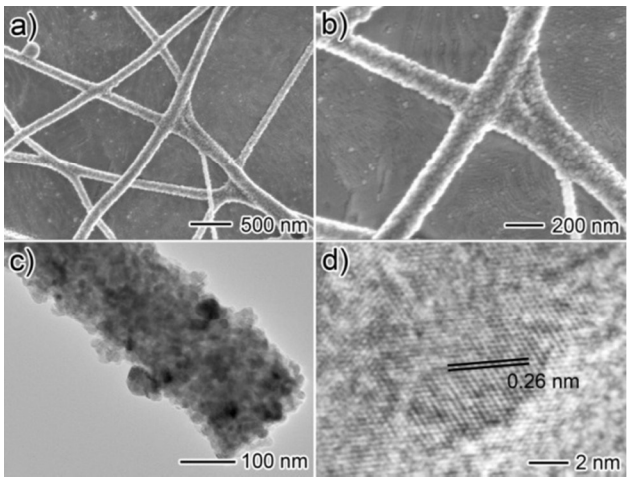


**Figure 1.** (a, b) SEM images of ZnO nanofibers deposited on the surface of silver foil with different magnifications. (c, d) TEM and HRTEM images of the as-prepared ZnO nanofibers.

measured lattice spacing of about 0.26 nm is attributed to the (002) interplanar spacing of ZnO (Figure 1d).[41,42] In addition, the electrospun ZnO nanofibers were also deposited on other metal foil surfaces, such as aluminum foil, and a similar morphology to that in Figure 1 was observed (Figure S1).

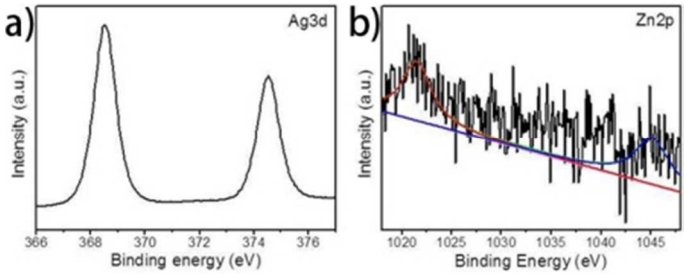


**Figure 2.** XPS spectra of ZnO nanofibers deposited on the surface of silver foil. (a) Ag3d; (b) Zn2p.

The cheimcal structure of the obtained ZnO nanfibers deoposited on the silver foil surface was characterized by XRD measurement, whose result is shown in Figure S2(a). As the content of ZnO was low, the XRD pattern showed only the typical peaks of silver. All the peaks could be indexed to Ag, indicating that the silver foil was not oxidized through a calcination process at 450°C. To obtain the XRD pattern of ZnO nanofibers, we increased the electrospinning time and then peeled off the electrospun PVP/zinc acewe membrane from substrate. After calcination, the XRD pattern showed the typical hexagonal wurtzite crystal structure of ZnO, demonstrating the successful preparation of ZnO nanofibers (Figure S2(b)). The chemical composition of the deposited ZnO nanofibers is revealed by X-ray photoelectron spectroscopy (XPS). The XPS spectrum showed that the $Ag3d_{5/2}$ and $Ag3d_{3/2}$ peaks appear at binding energies of 368.5 and 374.5 eV, respectively (Figure 2a). The splitting of the 3d doublet is 6.0 eV, indicating that the Ag foil is metallic silver.[43] In addition, the XPS spectrum also shows that $Zn2p_{3/2}$ and $Zn2p_{1/2}$ peaks appear at binding energies of 1021.4 and 1045.0 eV, respectively (Figure 2b).[43] Although the intensities of the Zn2p peaks are weak because of their lower density, the existence of ZnO nanofibers on the metallic silver foil may be concluded. The chemical structure of ZnO nanofibers deposited on the silver foil surface was also characterized by Raman spectrum. As shown in Figure S3, the characteristic peak at 236 $cm^{-1}$ is attributed to a $B_1^{low}$ mode, and the peak at 441 $cm^{-1}$ is associated with an $E_2^{high}$ mode of ZnO vibration. In addition, an $E_1^{low}$ mode at 583 $cm^{-1}$ related to the vibration of the oxygen atom is observed, indicating the existence of a wurtzite crystal phase of ZnO nanofibers on the silver foil surface.[44]

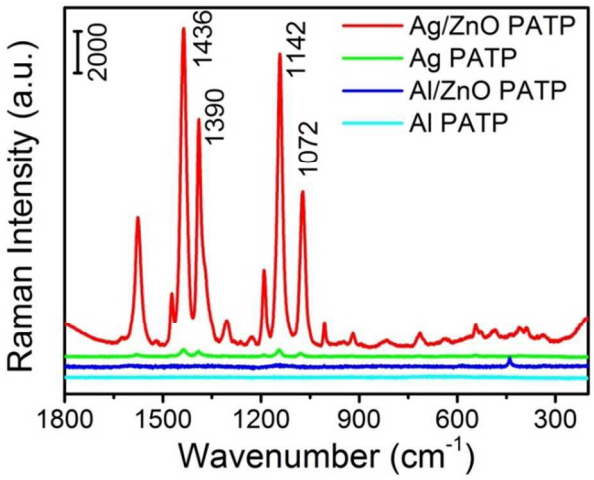


**Figure 3.** Raman spectra of PATP aqueous solution ($1\times10^{-5}$ M) on ZnO nanofibers deposited on the surface of silver foil (Ag/ZnO), silver foil (Ag), ZnO nanofibers deposited on aluminum foil (Al/ZnO), and aluminum foil (Al), respectively.

The ZnO nanofibers deposited on the silver foil surface have been used as an efficient SERS substrate, exhibiting greatly enhanced Raman signals. As shown in Figure 3, the Raman spectra exhibit several dominant strong peaks at around 1072, 1142, 1390, and 1436 $cm^{-1}$. The band at 1072 $cm^{-1}$ may be attributed to the $a_1$ band of PATP, while other characteristic bands at 1142, 1390, and 1436 $cm^{-1}$ are related to the $b_2$ vibration bands.[43] The presence of these PATP bands is consistent with previous reports on other SERS substrates.[43,45] For comparison, we have also evaluated the Raman spectra of PATP molecules deposited on silver and aluminum foil, as well as that of ZnO nanofibers deposited on aluminum foil. Much weaker PATP bands were observed on the surface of these substrates. These data indicate that the interaction between the ZnO nanofibers and silver foil surface plays an important role in Raman signal enhancement.

In the following study, concentration-dependent SERS spectra were obtained for PATP on ZnO nanofibers deposited on the silver foil surface (Figure 4). It was found that the SERS bands at 1072, 1142, 1390, and 1436 $cm^{-1}$ were clearly observed for PATP molecules at a concentration of $10^{-10}$ mol/L. At a concentration of $10^{-12}$ mol/L, the SERS intensity of the dominant PATP can still be observed in an enlarged SERS image. Thus, the as-prepared ZnO nanofibers deposited on the silver foil surface as a SERS substrate exhibit high sensitivity for the detection of PATP molecules even for concentrations as low as $10^{-12}$ mol/L.

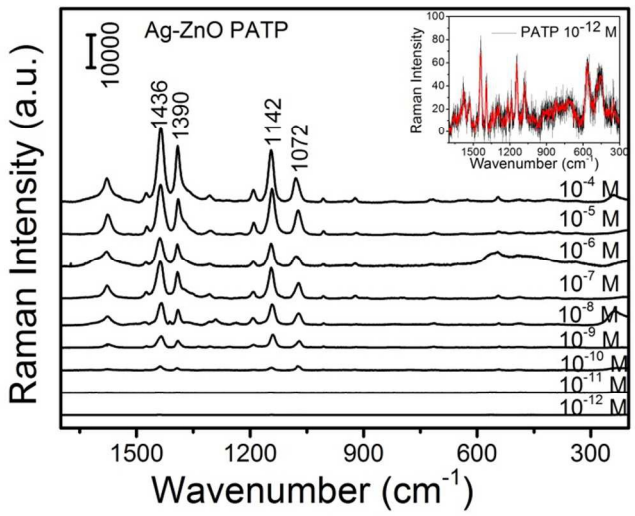


**Figure 4.** SERS spectra of PATP aqueous solution with different concentrations (from $10^{-4}$ to $10^{-12}$ mol/L) on ZnO nanofibers deposited on the surface of silver foil. The inset image shows the SERS spectrum of PATP aqueous solution with a concentration of $10^{-12}$ mol/L on ZnO nanofibers deposited on the surface of silver foil.

We also calculated the EF of the ZnO nanofibers deposited on the silver foil surface according to the following equation: [46]

$EF = (I_{SERS}/N_{SERS})/(I_0/N_0)$,

where $I_{SERS}$ and $I_0$ represent the SERS intensity of the band at 1072 $cm^{-1}$ ascribed to PATP adsorbed on the ZnO nanofibers/silver foil substrate and the Raman intensity of the band at 1083 $cm^{-1}$ attributed to 0.5 M PATP acidic solution, respectively. $N_{sers}$ represents the average number of adsorbed PATP molecules in the detection volume for the SERS experiment.

$N_{sers} = Ac_{surf}VN_A/A'$,

where $A$ is the area of the laser spot, $c_{surf}$ is the concentration of the determined PATP molecules, $V$ is the volume of the adsorbed molecules, $N_A$ is the Avogadro constant, and $A'$ is the area of modified substrate. $N_0$ is the average number of PATP molecules for the Raman measurement, which can be obtained by the equation:

$N_0 = c_0AhN_A$,

where $c_0$ represents the concentration of PATP for normal Raman measurement, $A$ and $N_A$ are the same as given above, $h$ is the effective focused depth. We assume that all molecules within the effective depth contribute to the whole Raman signal, and therefore, ignore the Raman signal from outside of the effective depth. The effective depth can be estimated to be about 6.9 μm. Based on the above data, the EF is calculated to be about $1.2 \times 10^8$, which is a high value for a semiconductor substrate.[18,20] This EF value is comparable to that of metallic substrates with EM enhancement.[47]

It has been reported that ZnO nanospheres show SERS spectra with an enhancement of about $10^3$, which is attributed to the CT resonance.[18] ZnO nanoparticles deposited on a 4,4-dimercaptostilbene-modified Au film also show enhanced Raman signals, with an EF value of about 4300.[48] The gap distance between the ZnO nanoparticles and gold film is relatively large for the existence of disulfide bonds, which leads to decreased EF. In our experiment, we have deposited the ZnO nanofiber precursors on the silver surface, followed by

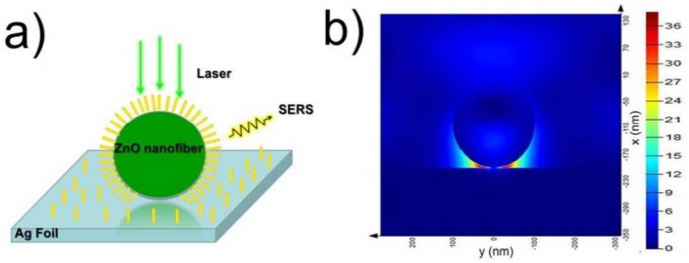


**Figure 5.** (a) Schematic of ZnO nanofibers deposited on the surface of silver foil functionalized with probes; (b) The distribution of the electric field for ZnO nanofibers deposited on the surface of silver foil calculated with FDTD simulation.

calcination, which enhances the interaction between ZnO nanofibers and the silver foil.The finite difference time domain (FDTD) has been used to investigate the enhancement mechanism. As shown in Figure 5b, the higher field enhancement is localized at the gap between ZnO nanofibers and silver foil, which indicates that the Raman enhancement in the SERS substrate based on the ZnO nanofibers deposited on the silver foil surface is due to the complementary optical properties of metal and semiconductor nanostructures. In general, optical excitations are observed in low-dimensional semiconductors because of the discrete levels in their conduction and valence bands. When ZnO nanofibers are deposited on the silver foil surface, strong interactions are generated between the electronic states in the semiconductor ZnO nanofibers and dielectric-confined EM modes in the silver foil. The high-index ZnO nanofibers excited continuous delocalized surface plasmons on the silver foil surface, resulting in localization of the electric field at the gap between ZnO nanofibers and silver foil. The exciton–plasmon interactions between the ZnO nanofibers and silver foil surface contribute to the enhanced scattering, which resulted in large EM field enhancement at the gap between ZnO nanofibers and silver foil for SERS experiments. Thus, it can be assumed that the EM coupling between the ZnO nanofibers and silver foil would lead to high SERS activity.

The distinct advantage of ZnO nanofibers deposited on the silver foil surface is their unique ability to monitor the reaction kinetics during the photocatalytic degradation of organic pollutants. In fact, the ZnO nanofibers showed enhanced photocatalytic activity toward the degradation of MB by combining ZnO nanofibers with silver foil, which might be due to the charge separation effect and an increase in the lifetime of the photogenerated excitons (Figure S4). In the presence of the deposited ZnO nanofibers, most of the MB molecules are photodegraded in 20 min, as investigated using UV-vis spectroscopy (Figure S5). Based on the above-mentioned results, the deposited ZnO nanofibers exhibit both excellent SERS properties and high photocatalytic performance; thus, we have used SERS spectroscopy to conduct monitoring of MB degradation, using the deposited ZnO nanofibers as both the SERS substrate and photocatalyst. The SERS monitoring measurements were performed in a liquid system using a 514.5 nm laser and the SERS signals were directly collected from the ZnO nanofiber substrate. The SERS spectra of the deposited ZnO nanofibers with the MB molecules at different time intervals after UV irradiation are shown in Figure 6. It is evident that the characteristic bands of MB appear before irradiation with UV light; for instance, the characteristic bands

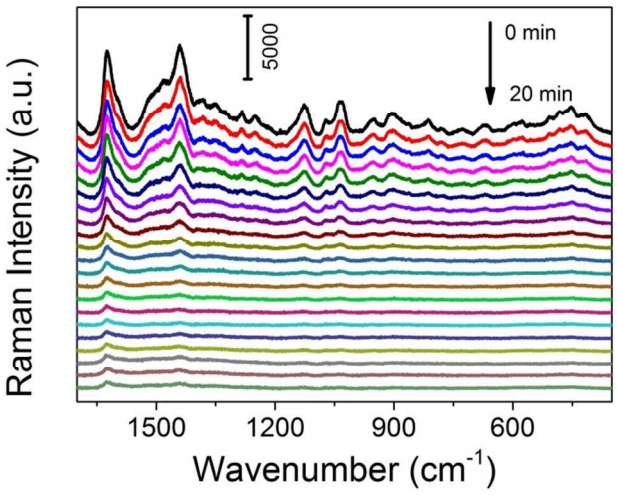


**Figure 6.** The change of SERS spectra for the photocatalytic degradation of MB on the substrate based on ZnO nanofibers deposited on the surface of silver foil. The time interval adopted for the spectral sequence is 1 min.

at 453, 577, 1031, 1127, 1441, 1510, and 1625 $cm^{-1}$ are attributed to C–N–C, C–S–C, C–H in-plane bending, $CH_3$ deformation, N–H bending, C–C stretching, and C–C ring stretching modes, respectively.[49] During photocatalysis under UV irradiation, the Raman intensity of these MB bands gradually decreases with increasing time, and no other new peaks emerge, which indicates the degradation of MB molecules in the presence of ZnO nanofibers deposited on the silver foil surface. The SERS spectra also showed that the characteristic peaks of MB almost disappeared after 20 min.

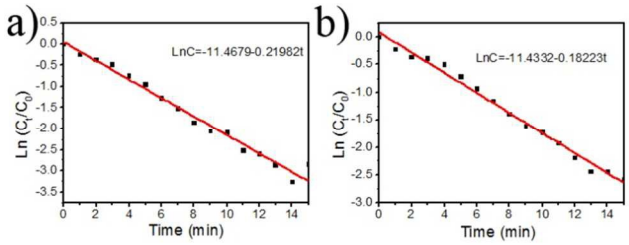


**Figure 7** The curves of the linear relationship between the concentration of MB and the reaction time according to the bands at (a) 1127 $cm^{-1}$ and (c) 1625 $cm^{-1}$.

In order to accurately and quantitatively determine the catalytic activity and the reaction kinetics of the photocatalytic process, we monitored the catalytic process using SERS based on the characteristic peak intensity. Figures 7a and b show the relationship between $\ln(C_t/C_0)$ and reaction time for the photodegradation of MB catalyzed by ZnO nanofibers deposited on the silver foil surface, wherein the ratio of $C_t$ to $C_0$ can be measured from the ratio of the intensity of the SERS peaks at times $t$ and 0, respectively, because the SERS intensity of MB is proportional to its concentration in the reaction system. As shown in Figure 7a and b, based on the time-dependent SERS intensity of MB molecules at 1127 and 1625 $cm^{-1}$, the relationship between the concentration and time from 1 to 15 min can be expressed as $\ln(C_{MB}) = -11.4679 - 0.21982t$ and $\ln(C_{MB}) = -11.4332 - 0.18223t$, respectively. These results indicate that MB photodegradation under UV light follows pseudo-first-order kinetics. In addition, the photocatalytic reaction rate constants are calculated to be about 0.2198 and 0.1822 $min^{-1}$, respectively. Other obvious characteristic SERS peaks of MB were also treated, and a similar linear relationship was obtained (Figure S6). It has been shown that the rate constant value seems to be higher than that obtained from UV-vis spectroscopy (Figure S5b), indicating that SERS provides information about the interface of the photocatalytic reaction process, while UV-vis only provides information about the reaction process in solution. Therefore, monitoring various kinds of catalytic reaction processes using the SERS technique offers attractive advantages compared with conventional spectroscopy techniques.

## Conclusions

In summary, we have fabricated a new type of highly sensitive SERS substrate based on ZnO nanofibers deposited on a silver foil surface through electrospinning followed by calcination process. The strong interactions between ZnO nanofibers and silver foil afford continuous delocalized surface plasmons, resulting in localization of the electric field at the gap between ZnO nanofibers and silver foil. Therefore, the exciton–plasmon interactions between ZnO nanofibers and the silver foil surface contribute to enhanced scattering, generating a large SERS enhancement. The as-prepared ZnO nanofibers deposited on the silver foil surface exhibit excellent photocatalytic activity towards pollutant (MB) degradation under UV irradiation because of the charge separation effect and increase in the lifetime of photogenerated excitons. Thus, it has been used as the SERS substrate for quantitative monitoring of pollutant degradation. We believe that such a strategy of fabricating semiconductor nanostructures on the surface of a metal film as both the SERS substrate and photocatalyst could be extended to other systems, which generates new features and applications.

## Acknowledgements

This work was supported by a Support Project to Assist Private Universities in Developing Bases for Research (Research Centre for Single Molecule Vibrational Spectroscopy) from the Ministry of Education, Culture, Sports, Science and Technology of Japan, the National Natural Science Foundation of China (nos. 21273091, 21327803, 21473068) and the Development Program of the Science and Technology of Jilin Province (20130522137JH). We also thank Prof. Xiaofeng Lu and Mr. Yan Tong for their help for the preparation of ZnO nanofibers, Mr. Hailong Wang for the FDTD simulation and their warmly discussions.

## Notes and references

[a] School of Science and Technology, Kwansei Gakuin Universty, 2-1 Gakuen, Sanda, Hyogo 660-1337, Japan, ozaki@kwansei.ac.jp
[b] State Key Laboratory of Supramolecular Structure and Materials, Jilin University; 2699#,Qianjin Steet, Changchun 130012, P. R. China, zhaob@jlu.edu.cn

† Electronic Supplementary Information (ESI) available: [details of any supplementary information available should be included here]. See DOI: 10.1039/b000000x/

1 M. Fleischmann, P. J. Hendra, A. J. McQuillan, *Chem. Phys. Lett.* **1974**, *26*, 163-166.

2 M. G. Albrecht, J. A. Creighton, *J. Am. Chem. Soc.* **1977**, *99*, 5215–5217.
3 D. L. Jeanmaire, R. P. Van Duyne, *J. Electroanal. Chem. Interf. Electrochem.* **1977**, *84*, 1-20.
4 K. Kneipp, M. Moskovits, H. Kneipp, Surface-Enhanced Raman Scattering-Physics and Applications, Springer, Heidelberg and Berlin, **2006**.
5 E. Le Ru, P. Etchegoin, Principles of Surface-Enhanced Raman Spectroscopy and Related Plasmonic Effects, Elsevier, Amsterdam, **2009**.
6 Y. Ozaki, K. Kneipp, R. Aroca, Frontiers of Surface-Enhanced Raman Scattering: Single Nanoparticles and Single Cells, John Wiley & Sons, Inc., **2014**.
7 S. Nie, S. R. Emory, *Science* **1997**, *275*, 1102-1106.
8 K. Kneipp, Y.Wang, H. Kneipp, L. T. Perelman, I. Itzkan, R. R. Dasari, M. S. Feld, *Phys. Rev. Lett.* **1997**, *78*, 1667-1670.
9 S. Schlücker, *Angew. Chem. Int. Ed.* **2014**, *53*, 4756-4795.
10 D. Y. Wu, J. F. Li, B. Ren, Z. Q. Tian, *Chem. Soc. Rev.* **2008**, *37*, 1025-1041.
11 S. E. J. Bell, N. M. S. Sirimuthu, *Chem. Soc. Rev.* **2008**, *37*, 1012-1024.
12 B. Sharma, R. R. Frontiera, A. I. Henry, E. Ringe, R. P. VanDuyne, *Mater. Today* 2012, *15*, 16-25.
13 L. Guerrini, D. Graham, *Chem. Soc. Rev,* **2012**, *41*, 7085-7107.
14 D. Lal, N. K. Grady, J. Kundu, C. S. Levin, J. B. Lassiter, N. J. Halas, *Chem. Soc. Rev.* **2012**, *37*, 898-911.
15. H. Y. Liang, Z. P. Li, W. Z. Wang, Y. S. Wu, H. X. Xu, *Adv. Mater.* **2009**, *21*, 4614-4618.
16. Y. Lu, G. L. Liu, L. P. Lee, *Nano Lett.* **2005**, *5*, 5-9.
17. M. V. Canamares, J. V. Garcia-Ramos, J. D. Gomez-Varga, C. Domingo, S. Sanchez-Cortes, *Langmuir* **2005**, *21*, 8546-8553.
18 Y. F. Wang, W. D. Ruan, J. H. .Zhang, B. Yang, W. Q. Xu, B. Zhao, J. R. Lombardi, *J. Raman Spectroscopy.* **2009**, *40*, 1072-1077.
19 Y. F. Wang, J. H. Zhang, H. Y. Jia, M. J. Li, J. B. Zeng, B. Yang, B. Zhao, W. Q. Xu, *J. Phys. Chem. C* **2008**, *112*, 996-1000.
20 L. B. Yang, X. Jiang, W. D. Ruan, B. Zhao, W. Q. Xu, J. R. Lombardi, *J. Phys. Chem. C* **2008**, *112*, 20095-20098.
21 Z. B. Lin, J. H. Tian, B. G. Xie, Y. G. Tang, J. J. Sun, G. N. Chen, B. Ren, B. W. Mao, Z. Q. Tian, *J. Phys. Chem. C* **2009**, *113*, 9224-9229.
22 L. G. Quagliano, J. Am. Chem. Soc. 2004, 126, 7393-7398.
23 R. Livingstone, X. Zhou, M. C. Tamargo, J. R. Lombardi, J. Phys. Chem. C 2010, 114, 17460-17464.
24 Z. B. Lin, B. G. Xie, J. H. Tian, Y. G. Tang, J. J. Sun, G. N. Chen, B. Ren, B. W. Mao, Z. Q. Tian, J. Electroanal. Chem. 2009, 636, 74-79.
25 P. Tarakeshwar, J. L. Palma, D. Finkelstein-Shapiro, A. Keller, I. Urdaneta, M. Calatayud, O. Atabek, V. Mujica, J. Phys. Chem. C **2014**, *118*, 3774-3782.
26 J. R. Lombardi, R. L. Birke, *J. Phys. Chem. C* **2014**, *118*, 11120-11130.
27 W. Ji, Y. Wang, I. Tanabe, X. Han, B. Zhao, Y. Ozaki, *Chem. Sci.* **2015**, *6*, 342-348.
28 X. Ling, L. M. Xie, Y. Fang, H. Xu, H. L. Zhang, J. Kong, M. S. Dresselhaus, J. Zhang, Z. F. Liu, *ACS Nano* **2010**, *10*, 553-561.
29 W. G. Xu, N. N. Mao, J. Zhang, *Small* **2013**, *9*, 1206-1224.
30 N. P. Dasgupta, J. Sun, C. Liu, S. Brittman, S. C. Andrews, J. Lim, H. Gao, R. Yan, P. D. Yang, *Adv. Mater.* **2014**, *26*, 2137-2184.
31 W. Lu, C. M. Lieber, *J. Phys. D: Appl. Phys.* **2006**, *39*, R387-R406.
32 R. B. Jiang, B. X. Li, C. H. Fang, J. F. Wang, *Adv. Mater.* **2014**, *26*, 5274-5309.
33 M. Achermann, *J. Phys. Chem. Lett.* **2010**, *1*, 2837-2843.
34 C. O. Aspetti, R. Agarwal, *J. Phys. Chem. Lett.* **2014**, *5*, 3768-3780.
35 W. Song, Y. X. Wang, B. Zhao, *J. Phys. Chem. C* **2007**, *111*, 12786-12791.
36 W. Song, X. X. Han, L. Chen, Y. M. Yang, B. Tang, W. Ji, W. D. Ruan, W. Xu, B. Zhao, Y. Ozaki, *J. Raman Spectrosc.* **2010**, *41*, 907-913.
37 G. Sinha, L. E. Depero, I. Alessandri, *ACS Appl. Mater. Interf.* **2011**, *3*, 2557-2563.
38 H. Kim, K. M. Kosuda, R. P. VanDuyne, P. C. Stair, *Chem. Soc. Rev.* **2010**, *39*, 4820-4844.
39 C. Y. Wen, F. Liao, S. S. Liu, Y. Zhao, Z. H. Kang, X. L. Zhang, M. W. Shao, *Chem. Commun.* **2013**, *49*, 3049-3051.
40 M. Muniz-Miranda, *Appl. Catal. B: Environ.* **2014**, *146*, 147-150.
41 J. L. Yu, Y. F. Lai, Y. Z. Wang, S. Y. Cheng, Y. H. Chen, *J. Appl. Phys.* **2014**, *115*, 033505.
42 Y. F. Lai, Y. Z. Wang, S. Y. Cheng, J. L. Yu, *J. Electron. Mater.* **2014**, *43*, 2676-2682.
43 W. Song, Y. Wang, H. L. Hu, B. Zhao, *J. Raman Spectrosc.* **2007**, *38*, 1320-1325.
44 S. Kuriakose, V. Choudhary, B. Satpati, S. Mohapatra, *Phys. Chem. Chem. Phys.* **2014**, *16*, 17560-17568.
45 Z. Mao, W. Song, X. X. Xue, W. Ji, Z. S. Li, L. L. Chen, H. J. Mao, H. M. Lv, X. Wang, J. R. Lombardi, B. Zhao, *J. Phys. Chem. C* **2012**, *116*, 14701-14710.
46 H. Y. Zhao, J. Jin, W. J. Tian, R. Li, Z. Yu, W. Song, Q. Cong, B. Zhao, Y. Ozaki, *J. Mater. Chem. A* **2015**, *3*, 4330-4337.
47 L. M. Tong, T. Zhu, Z. F. Liu, Chem. Soc. Rev. 2011, 40, 1296-1304.
48 L. Li, T. Hutter, A. S. Finnemore, F. M. Huang, J. J. Baumberg, S. R. Elliott, U. Steiner, S. Mahajan, *Nano Lett.* **2012**, *12*, 4242-4246.
49 C. M. Ruan, W. Wang, B. H. Gu, *J. Raman Spectrosc.* 2007, *38*, 568-573.

# Fabrication of a highly sensitive surface-enhanced Raman scattering substrate for monitoring of the catalytic degradation of organic pollutants

Wei Song,[a,b] Wei Ji,[a] Sanpon Vantasin,[a] Ichiro Tanabe,[a] Bing Zhao*[b] and Yukihiro Ozaki*[a]

**Graphical abtract**

We have described a simple and reliable electrospinning technique combined with calcination process to fabricate ZnO nanofibers deposited on the silver foil surface. The ZnO nanofibers on the surface of silver foil can be used as both photocatalyst and efficient SERS substrate for monitoring the catalytic degradation process of organic pollutants.